Environmental Science & Technology

pubs.acs.org/est

Article

Persistence of Human Norovirus (GII) in Surface Water: Decay Rate Constants and Inactivation Mechanisms

Lauren C. Kennedy, Veronica P. Costantini, Kimberly A. Huynh, Stephanie K. Loeb, Wiley C. Jennings, Sarah Lowry, Mia C. Mattioli, Jan Vinjé, and Alexandria B. Boehm*

Cite This: *Environ. Sci. Technol.* 2023, 57, 3671−3679

Read Online

ACCESS | Metrics & More | Article Recommendations | Supporting Information

ABSTRACT: Human norovirus (HuNoV) is an important cause of acute gastroenteritis and can be transmitted by water exposures, but its persistence in water is not well understood. Loss of HuNoV infectivity in surface water was compared with persistence of intact HuNoV capsids and genome segments. Surface water from a freshwater creek was filter-sterilized, inoculated with HuNoV (GII.4) purified from stool, and incubated at 15 or 20 °C. We measured HuNoV infectivity via the human intestinal enteroid system and HuNoV persistence via reverse transcription-quantitative polymerase chain reaction assays without (genome segment persistence) or with (intact viral capsid persistence) enzymatic pretreatment to digest naked RNA. For infectious HuNoV, results ranged from no significant decay to a decay rate constant ("*k*") of 2.2 day^{-1}. In one creek water sample, genome damage was likely a dominant inactivation mechanism. In other samples from the same creek, loss of HuNoV infectivity could not be attributed to genome damage or capsid cleavage. The range in *k* and the difference in the inactivation mechanism observed in water from the same site could not be explained, but variable constituents in the environmental matrix could have contributed. Thus, a single *k* may be insufficient for modeling virus inactivation in surface waters.

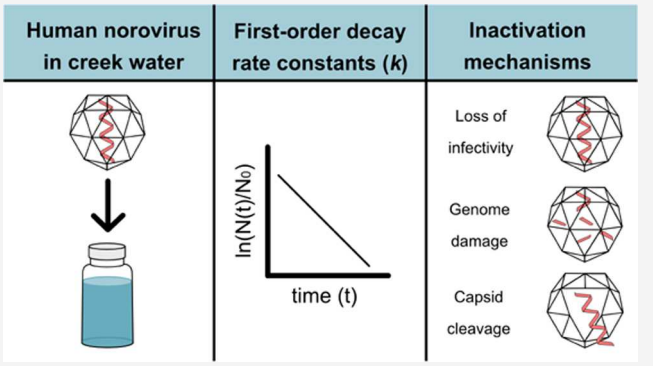

KEYWORDS: *virus, creek water, genome integrity, capsid integrity*

INTRODUCTION

Human norovirus (HuNoV) is a leading cause of acute gastroenteritis globally[1−4] and an important contributor to recreational waterborne illness.[5−8] HuNoV can be detected in environmental water,[5−7,9−13] and a recent systematic review and meta-analysis detected HuNoV in 31.7% of global environmental water samples (n = 9970).[14] HuNoV is exclusively measured in the environment using molecular methods like reverse transcription-quantitative polymerase chain reaction (RT-qPCR), which detect viral genomic RNA (gRNA) from both noninfectious and infectious viruses. Depending on the environmental conditions, gRNA can persist for extended periods in environmental water.[15,16] Thus, it is uncertain what proportion of detected gRNA is from infectious virus. The relationship between the presence of HuNoV gRNA compared to infectious virus persistence (i.e., the amount of time each remains detectable) is not well understood in surface water.

Two systematic reviews have summarized the persistence of nonenveloped and enveloped viruses in surface waters.[17,18] Those reviews found that water temperature was one of the most important factors affecting decay (i.e., the loss of virus molecular signal) and resulting first-order decay rate constants. At the time of those reviews, there were only two studies[19,20] with available first-order decay rate constants for HuNoV (quantified via RT-qPCR). The only other data available for caliciviruses used murine norovirus (quantified via RT-qPCR and/or culture methods).[20−22] Since then, additional studies have been published describing inactivation (i.e., loss of infectious virus) of murine norovirus using cell culture (RAW-264.7)[23] and HuNoV using cell culture (human intestinal enteroid (HIE) cells).[24,25] Given the importance of norovirus globally as an etiology of acute gastrointestinal illness, there is an urgent need to better understand its inactivation in water.

Enteric virus inactivation in water can be affected by physical (e.g., sunlight, temperature), chemical (e.g., pH, salinity), and biological (e.g., predation by protozoa, bacterial activity) factors.[26,27] These factors can cause loss of virus infectivity from damage to its genome or proteins, including capsid

Received: December 21, 2022
Revised: February 8, 2023
Accepted: February 10, 2023
Published: February 22, 2023

https://doi.org/10.1021/acs.est.2c09637
Environ. Sci. Technol. 2023, 57, 3671−3679

Table 1. Details of Experiments Assessing the Persistence of HuNoV in Filter-sterilized Water Collected from San Pedro Creek[a]

experiment	temp. (°C)	rep.	start date (m/y)	San Pedro Creek water collection date (m/d/y)	filter pore size (μm)	HuNoV accession #	time points (day)	quantification methods
15-1	15	1	08/2019	07/22/2019	0.1	MK764019	0, 1, 7, 14, 21, 28	HIE assay, RT-qPCR
15-2	15	2	02/2020	01/14/2020	0.1	MK764019	0, 1, 3, 5	HIE assay, RT-qPCR, ET-RT-qPCR
20-1	20	1	01/2022	11/8/2021	0.22	OL913976	0, 1, 7	HIE assay, RT-qPCR
20-2	20	2	02/2022	11/8/2021	0.22	OL913976	0, 1, 7, 14, 21, 28	HIE assay, RT-qPCR, ET-RT-qPCR

[a]The experiment name is provided in the experiment column. Remaining columns provide the temperature (temp.) at which the experiment took place, the replicate number (Rep.), the start date of the experiment in the laboratory, the date on which the creek water was collected, the pore size of the filter used to filter-sterilize the water, the accession # for the genome sequence of the HuNoV strain used to inoculate the experiments, the time points at which HuNoV was quantified after inoculation (day 0), and the last column on the right provides the methods used to quantify HuNoV.

cleavage.[26,28,29] For HuNoV, in particular, the loss of infectivity is difficult and costly to assess using cell lines.[30] In some studies, molecular methods have been used to estimate viral infectivity through whole-genome persistence (i.e., extrapolating the damage incurred by long segment(s) of the viral RNA genome to estimate that of the whole genome) and intact viral capsid persistence (i.e., pretreating samples to remove the genetic material that is not shielded by a viral capsid or capturing and concentrating intact viral capsids).[29,31−38] These methods can also provide insight into inactivation mechanisms by comparing if the capsids were cleaved or if the genome was destroyed over time at a comparable rate to loss of infectivity. However, few studies have assessed HuNoV capsid and genome damage concurrently in environmental contexts.[35,37] Mechanistic studies of HuNoV inactivation in environmental waters are needed.

To fill these knowledge gaps, we aim to measure the loss of infectivity of HuNoV in surface water (measured by viral replication using the HIE system), to compare the loss of infectivity to the intact HuNoV capsid and HuNoV genome persistence, and to assess the mechanism of inactivation for different surface water conditions. The first-order decay rate constants for HuNoV reported in this study are valuable parameters for fate and transport models. This work also provides insight into the inactivation mechanisms of HuNoV in surface water.

METHODS

Overview. Laboratory microcosm experiments were conducted to measure the loss of infectivity of HuNoV suspended in filter-sterilized surface water from a freshwater creek incubated at 15 and 20 °C, to compare the persistence of infectious HuNoV to that of the intact viral capsid and HuNoV genome, and to infer the cause of the loss of infectivity. Experiments were conducted by adding HuNoV purified from stool filtrates to filter-sterilized creek water, incubating the waters in the dark at 15 and 20 °C. Filter-sterilized creek water was used to quantify the effects of small (<0.22 μm) biotic (e.g., enzymatic) and abiotic factors on the decay rate constants of HuNoV. The 15 and 20 °C incubation temperatures represent the range of annual average water temperatures in freshwater bodies in the United States.[39] The infectivity of the virus, as well as the intact viral capsid and HuNoV genome signal decay, was followed over time. For simplicity, the experiments are referred to as 15-1, 15-2, 20-1, and 20-2 to indicate the temperature of the experiment and the replicate number (Table 1).

Preparation of HuNoV Inoculant. Human stool samples positive for HuNoV were used to prepare HuNoV inoculants. Briefly, each stool sample was diluted into autoclaved phosphate-buffered saline (Fisher Scientific), sonicated to homogenize the sample, centrifuged to remove debris, and sequentially filtered through four filters (smallest pore size 0.2 μm) to purify the inoculant. Though we did not characterize viral aggregates in the inoculate, sonication has been shown to reduce virus aggregation.[40] The HuNoV inoculant was stored at −80 °C until use. The inoculant was quantified via RT-qPCR prior to experiments. Additional details are provided in the Supporting Information (SI).

Creek Water Collection. Surface water was obtained from San Pedro Creek in Pacifica, CA (37.59°N, −122.5°W) using sterile technique on three different dates during dry weather conditions. Water was collected three times (creek water A: July 2019, creek water B: January 2020, and creek water C: November 2021). Raw water samples were visually clear. An aliquot of water was filtered using 0.22 (Experiments 20-1 and 20-2) or 0.1 μm (Experiments 15-1 and 15-2) pore size filters and stored at 4 °C until use in the experiments (between 1 and 4 months). Filtration was applied in place of other sterilization methods, such as autoclaving, to avoid altering the biotic (e.g., enzymatic) and abiotic components remaining in the water. Multiple samples of creek water were collected intentionally to reduce the time between sample collection and use in experiments and to include intrinsic surface water quality variability in the experimental design.

The salinity and temperature of the raw water were measured at the time of collection. After the sample was transported on ice and filtered, turbidity, pH, UV−vis absorbance, intracellular and extracellular adenosine triphosphate (ATP) concentrations were measured. No water quality data were collected for one sample date, but previous research at this site indicated stable bulk water quality characteristics during dry weather.[41] Additional details are provided in the SI.

Experimental Setup. Experiments followed the infectivity of HuNoV, as well as the signal decay of the intact viral capsid and RNA genome in creek water (15-1, 15-2, 20-1, and 20-2; Table 1 and Figure S1). For all experiments, creek water was inoculated with HuNoV GII.4 Sydney strain such that the starting concentration was between $2.4 \times 10^5 \pm 4.3 \times 10^4$ and $7.1 \times 10^5 \pm 3.5 \times 10^4$ gene copies per mL (gc/mL) of HuNoV (error is the standard deviation). Water samples were aseptically divided into 1 mL aliquots and stored in the dark at 15 °C (15-1 and 15-2) or 20 °C (20-1 and 20-2). One 1 mL aliquot was sacrificed at each time point (Table 1); time points were generally 7 days apart and the duration of the

https://doi.org/10.1021/acs.est.2c09637
Environ. Sci. Technol. 2023, 57, 3671−3679

experiments was 5 and 28 days. Experiments 20-1 and 20-2 were each completed with replicate 1 mL aliquots at each time point (Figure S1). At each time point, each sacrificed aliquot was divided into two: one subaliquot was used to evaluate HuNoV infectivity in HIE cells and the other to evaluate HuNoV decay using five different RT-qPCR assays. Additional details can be found in the SI.

The concentrations of one short segment of gRNA commonly used to quantify HuNoV in the environment (89 nt, hereafter referred to as "ORF"), and four different long segments (~500 nt) of gRNA were measured at each time point using RT-qPCR. The combined damage incurred by the long genome segments was extrapolated to estimate that of the whole genome.[31] For the short-genome segment dsDNA assay, the R^2 and efficiency of the master standard curve were 0.99 and 84.3%, respectively (Table S7). Across all long genome segment dsDNA assays used on experimental samples, the R^2 and efficiency of the master standard curves ranged from 0.93 to 1 and 76.6 to 100.1%, respectively (Table S7). In two experiments (15-2 and 20-2), RT-qPCR was completed with samples pretreated with RNase I (Thermo Fisher Scientific; enzyme-treated RT-qPCR; ET-RT-qPCR) to eliminate gRNA not protected within an intact viral capsid.[42−44] The details of these methods are provided below.

Positive HuNoV stool samples were limited and so different HuNoV stool filtrates were used for experiments 15-1 and 15-2 (accession #MK764019) and experiments 20-1 and 20-2 (accession #OL913976). Although the genomic sequences of these HuNoV strains have 97.7% pairwise nucleotide identity and were genotyped as GII.4 Sydney, separate RT-qPCR assays targeting long segments of each genome had to be designed for use with each (see details below).

HuNoV Infectivity. HuNoV infectivity was assessed via *in vitro* HIE assay as previously described.[25,45] Importantly, this method uses RT-qPCR to assess viral replication in HIE cells by comparing the increase of norovirus genomic copies at 72 h postinfection with the genomic copies at 1 h postinfection (no amplification). Additional details are provided in the SI.

Enzymatic Pretreatment. A subset of samples from the experiments were subjected to enzymatic pretreatment to digest gRNA not protected by an intact viral capsid. Two-hundred and fifty microliters of the sample was treated with 0.1 U/μL of RNase I (Thermo Fisher) with a 30 min (20-2) or 15 min (15-2) incubation period at 37 °C, and RNA extractions immediately followed the incubation period. The validity of this method was tested using creek water inoculated with intact HuNoV and naked gRNA.

RNA Extraction and cDNA Synthesis. RNA was extracted from 200 μL aliquots of samples using a Qiagen AllPrep DNA/RNA kit (Qiagen) without bead beating following manufacturer specifications. The extracted RNA was incubated with 60 μL of nuclease-free water for 5 min at room temperature before elution. A portion of the RNA extract was immediately reverse-transcribed to cDNA with an iScript cDNA synthesis kit (Bio-Rad), as per manufacturer specifications, with 20 μL reactions and 15 μL of template RNA. The cDNA and the remaining RNA extract were stored at −80 °C until molecular testing. Extraction controls included filter-sterilized creek water without (negative) and with (positive) seeded intact HuNoV.

RT-qPCR Assays. The Environmental Microbiology Minimum Information Guidelines[46] were followed. A previously developed probe-based assay was used[47] in addition to intercalating dye-based assays described below. The probe-based assay targeted a short region of the HuNoV GII genome (89 nt) located at the ORF1-ORF2 junction ("ORF"). The ORF assay was used in a one-step format using RNA as the template.

Intercalating dye-based (EvaGreen qPCR dye, Biotium) assays were designed that target long segments (~500 nt) of the specific HuNoV genomes used as inoculants in the study. A total of four assays targeting distinct regions of the RNA genome were designed for each of the two HuNoV strains. For experiments 15-1 and 15-2, the four assays (MK1, MK3, MK5, and MK7) in total captured about 27% of the HuNoV genome. In total, the targeted genome segments covered 2030 nt of the 7511 nt genome. For experiments 20-1 and 20-2, the four assays (OL1b, OL3a, OL5a, and OL7b) in total captured about 26% of the HuNoV genome. In total, the targeted genome segments covered 1957 nt of the 7560 nt genome. All intercalating dye-based assays used cDNA as the template. Details of assay design and validation methods are in the SI.

For RT-qPCR plates that included experimental samples, standard curves and no-template controls were completed in technical duplicate, and standard curves were combined into master standard curves to calculate quantities (Table S7). Samples were considered below the limit of quantification and were considered not detectable if they had a threshold cycle (Ct) value greater than the Ct value of the lowest quantity standard for each assay. Negative and positive extraction and PCR controls were included. Negative controls were considered negative if they did not amplify or amplified at a Ct value greater than the highest Ct value in the master standard curve. A subset of samples were tested for inhibition by comparing no dilution to a 1:5 dilution factor of samples on the same RT-qPCR plate, and it was determined that there was no inhibition. All RNA and cDNA templates were added undiluted to the reactions. Additional details of the master-mix, cycling conditions, instrumentation, assay performance, standard curves, and inhibition testing for all assays are provided in the SI (Tables S2−S7and Figures S4, S6, and S7).

Data Analysis. Data analysis was completed in R (v4.1.3). The observed first-order decay rate constants ("k values") were calculated based on eq 1,[48] where N_0 and $N(t)$ are the amount of HuNoV gc/mL on day 0 or at time (t), respectively, β_0 represents the intercept, and ε represents the error. The k values were calculated by plotting $\ln(N(t)/N_0)$ as a function of time for each experiment and calculating the slope, its standard error, and its p value. Each data point represented the arithmetic mean of technical triplicate (HIE assay) or technical duplicate (all other assays) measurements. Note that the HIE assay units are reported as gc/mL despite the fact that it is an infectivity assay because RT-qPCR was used to measure the number of infectious particles produced in HIE cells 72 h postinfection.[45] For experiments 20-1 and 20-2, the data points represent the arithmetic mean of the experimental duplicates. $\ln(N(t)/N_0)$ values that were not quantifiable were excluded from the linear regression (Tables S5 and S6).

$$\ln\left(\frac{N(t)}{N_0}\right) = \beta_0 - kt + \varepsilon \tag{1}$$

Multiple Linear Regression Analysis. The effects of incubation temperature (20 °C compared to 15 °C) and of genome segment length on HuNoV persistence were investigated using multiple linear regression with interaction

https://doi.org/10.1021/acs.est.2c09637
Environ. Sci. Technol. 2023, 57, 3671−3679

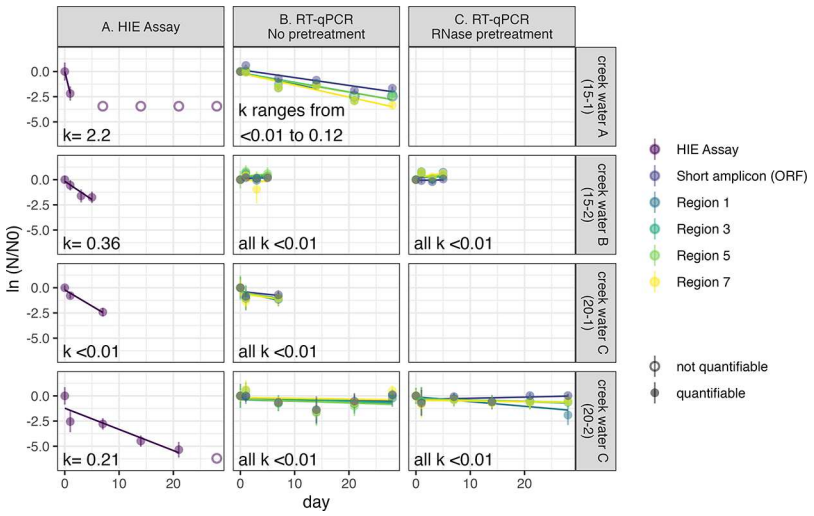

Figure 1. Persistence of HuNoV in filter-sterilized surface water incubated at 15 and 20 °C under dark conditions over time assessed via HIE assay (A) and via RT-qPCR assays targeting short and long HuNoV genome segments in different regions of the genome (color) with (B) and without (C) RNase pretreatment. Decay rate constants (k values) are provided in each plot (units are day^{-1}); k values that were not significantly different from 0 are denoted as "k < 0.01." Error bars depict the standard deviation of technical replicates, except for experiments 20-1 and 20-2 for which they depict the standard deviation of experimental replicates. RNase pretreatment was not completed for experiments 15-1 and 20-1.

effects.[49] The effect of temperature on the persistence of infectious HuNoV or HuNoV genome segments in creek water was tested using a multiple linear regression model of $\ln(N(t)/N_0)$ versus time (t; days), where time was allowed to interact with a dummy variable for the 20 °C temperature condition (R) and β_1, β_2, and β_{12} represent coefficients (eq 2). For HuNoV genome segments, the effect of amplicon length on the persistence of HuNoV genome segments in creek water was tested using a similar multiple linear regression model, where time was allowed to interact with a dummy variable for long genome segments (L;~500 nts) (eq 3).

$$\ln\left(\frac{N(t)}{N_0}\right) = \beta_0 + \beta_1 t + \beta_2 R + \beta_{12} tR + \varepsilon \tag{2}$$

$$\ln\left(\frac{N(t)}{N_0}\right) = \beta_0 + \beta_1 t + \beta_2 L + \beta_{12} tL + \varepsilon \tag{3}$$

Genome-Wide Decay Rate Constant Calculation. Genome-wide decay rate constants were calculated as described previously.[31,35] Briefly, the HuNoV whole-genome persistence was estimated by extrapolating the damage incurred by four long segments of the HuNoV genome (in regions 1, 3, 5, and 7) to that of the whole genome, assuming single-hit inactivation kinetics for HuNoV. It should be noted that results from previous studies of virus inactivation suggest that a single-hit model of inactivation for virus genomic damage may be an oversimplification for some conditions.[35,50] The proportion of the HuNoV genome that persisted ($N_{G,t}/N_{G,0}$) was estimated using eq 4, where $N_{i,0}$ and $N_{i,t}$ are the amount of HuNoV gc/mL on day 0 or at time (t), respectively, for each long RT-qPCR target, i. The genome-wide decay rate constant (k_G) was calculated by plotting $\ln(N_{G,t}/N_{G,0})$ as a function of time for each experiment and calculating the slope, its standard error, and its p value (eq 5). The p values herein are regression coefficient p values from eqs 1−3, or 5. The smallest first-order decay rate constant obtained in this study that was significantly different from zero was 0.078 day^{-1}, so first-order decay rate constants that were not significantly different from 0 were substituted with <0.01 day^{-1} on plots. The code and dataset are available at the Stanford Digital Repository (https://doi.org/10.25740/tr061rz9792)

$$\frac{N_{G,t}}{N_{G,0}} = \left[\prod_{i=1}^{n} \frac{N_{i,t}}{N_{i,0}}\right]^{\text{genome length/total length of n RT-qPCR targets}} \tag{4}$$

$$\ln\left(\frac{N_{G,t}}{N_{G,0}}\right) = \beta_0 - k_G t + \varepsilon \tag{5}$$

RESULTS

The persistence of infectious HuNoV (GII.4), short and long HuNoV genome segments, and intact HuNoV capsids was assessed in fresh, filter-sterilized surface waters from San Pedro Creek at two incubation temperatures (15 and 20 °C; Figure 1). The salinity of the raw water was <0.3 ppt, and the water temperature was between 10 and 20 °C upon collection (Table S1). After filter sterilization, the pH was 7.6, the total ATP was 2.7×10^{-2} nM, and the intracellular ATP was 9.0×10^{-4} nM for the creek water sample tested. The water was clear, as indicated by the turbidity (<1 NTU) and the absorbance spectra in Figure S2. Additional details are provided in the SI.

Quality Assurance/Quality Control. We included controls to confirm that the RNase pretreatment and RT-qPCR assays worked as intended. After RNase pretreatment, the concentration of intact HuNoV (i.e., the signal from RT-qPCR after RNase digestion) seeded into water did not change substantially: The concentration was $1.5 \times 10^5 \pm 5.0 \times 10^4$ gc/mL before pretreatment with RNase compared to $1.1 \times 10^5 \pm 4.3 \times 10^4$ gc/mL after pretreatment (as measured by ORF, where the error is the standard deviation). However, the concentration of naked HuNoV gRNA seeded into the same water diminished: The concentration was $1.3 \times 10^3 \pm 6.2 \times 10^2$ gc/mL before pretreatment with RNase compared to no amplification after pretreatment (as measured by ORF, where error is the standard deviation). Three of 58 RT-qPCR no-

https://doi.org/10.1021/acs.est.2c09637
Environ. Sci. Technol. 2023, 57, 3671−3679

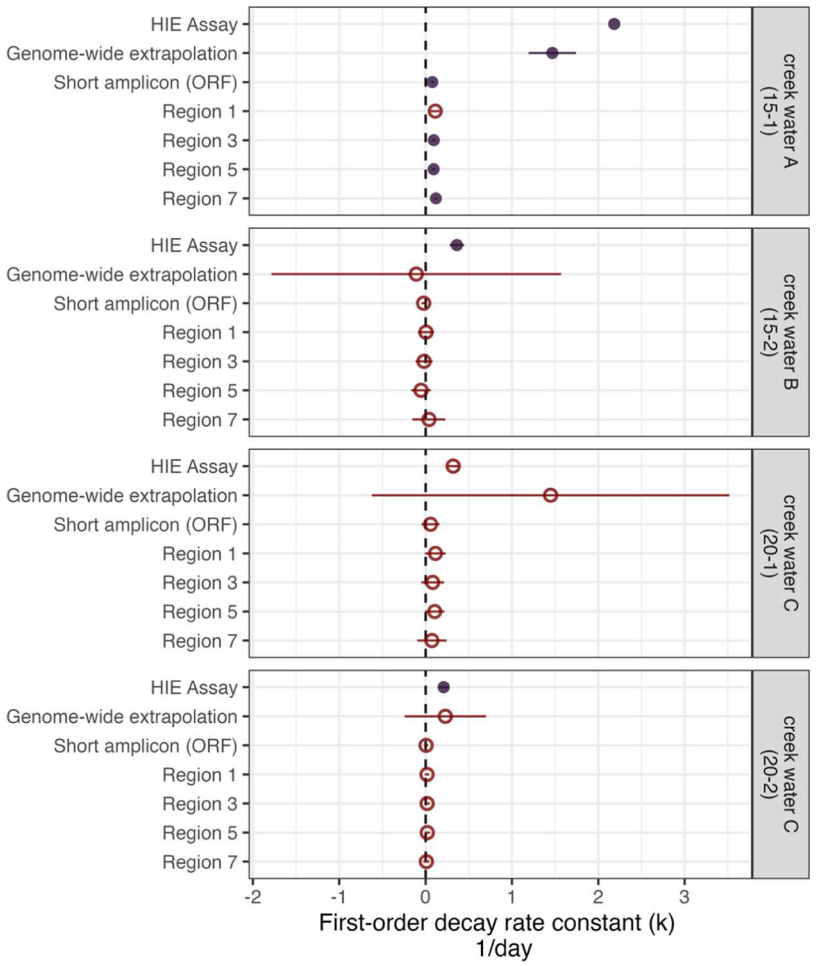

Figure 2. Variation in k values by experiment. The dashed vertical dashed line denotes 0. Error bars depict the standard error of the first-order decay rate constant (k). The red, open points are not significantly different from 0. No error bars are shown for experiment 15-1 HIE assay because only two data points were used to calculate k and an error could not be calculated.

template controls amplified to produce Ct values within the range of those produced by running the standard curve, but these Ct values were at least 3 Ct higher than any other experimental sample on the plate and, based on our calculations, were at concentrations too low to affect concentrations of the experimental samples on the plate (see the SI). Thus, the data from these two plates were retained in our analyses. Additional positive and negative analytical and preanalytical controls (positive and negative extraction controls, and positive and negative RT-qPCR controls) gave expected positive and negative results, confirming the lack of contamination during RNA extraction and RT-qPCR.

Persistence of Infectious HuNoV. The first-order decay rate constant, or "k value," measured in experiment 15-1 was 2.2 day^{-1}, which is larger than those observed in the other experiments, including experiment 15-2 (Figure 2). Note that no standard error value can be provided for this k value because only two data points in the time series were quantifiable (Figure 1). The k values were similar for experiments 15-2 and 20-2 at 0.36 ± 0.083 and 0.21 ± 0.056 day^{-1}, respectively (Table S11; the standard error on the slope of the regression is the error used throughout, unless otherwise noted). No significant decay was observed for experiment 20-1 (0.32 ± 0.06 day^{-1}; p = 0.12). The k value observed for experiment 15-1 was larger in magnitude compared to that of all other experiments, including 15-2 (2.2 compared to 0.36 ± 0.083 day^{-1}; Table S11). Based on the multiple linear regression, the HuNoV inactivation rate constants of replicate experiments were not significantly different for the 20 °C condition compared to that of the 15 °C condition (β_{12} in eq 2 was not significantly different from 0; $p > 0.05$; Table S8).

Persistence of the HuNoV Genome. The persistence of one short (89 nt) and four long (~500 nt) segments of the HuNoV genome was assessed via RT-qPCR. Short and long genome segments were more persistent (k values were significantly smaller) compared to infectious HuNoV assessed via the HIE assay (Figure 1). For experiment 15-1, the long genome segment k values were similar to that of the short genome segment, ORF: the k values assessed via RT-qPCR were 0.095 ± 0.023, 0.093 ± 0.020, and 0.12 ± 0.016 day^{-1} for region 3, region 5, and region 7, and 0.078 ± 0.016 day^{-1} for ORF (Table S11 and Figure 2). No significant decay was observed for all other experiments and the region 1 amplicon for experiment 15-1 ($p > 0.05$; Figure 2).

We used multiple linear regression models to test if 20 °C compared to 15 °C incubation temperature condition and if genome segment length affected the persistence of HuNoV genome segments (Tables S9 and S10). The genome segment persistence in the 20 °C condition was significantly different from that of the 15 °C condition (β_{12} in eq 2 was significantly different from 0; $p < 0.0001$). HuNoV genome segments

https://doi.org/10.1021/acs.est.2c09637
Environ. Sci. Technol. 2023, 57, 3671−3679

persisted longer at 20 °C compared to 15 °C: $\ln(N(t)/N_0)$ decreased by 0.021 units for each additional day incubated at 20 °C compared to 0.10 units at 15 °C. The persistence of HuNoV long genome segments was not significantly different from that of short genome segments (β_{12} in eq 3 was not significantly different from 0; $p > 0.05$).

The four RT-qPCR assays targeting long segments of the HuNoV genome were used to quantify overall HuNoV genome persistence by determining a genome-wide k value for each experiment. The genome-wide k value for experiment 15-1 (1.5 ± 0.27 day^{-1}) was larger than those determined with individual long RT-qPCR assays (0.093 ± 0.020 to 0.12 ± 0.016 day^{-1}) and similar in magnitude to the k value assessed via the HIE assay (2.2 day^{-1}; Figure 2). No significant decay was observed for the other experiments (genome-wide k values were not significantly different from 0; Figure 2 and Table 2).

Table 2. Genome-Wide First-Order Inactivation Rate Constants (k_G) for Each Experiment[a]

experiment	temperature (°C)	k_G (day^{-1})	standard error	p value
15-1	15	1.5	0.27	0.0059
15-2	15	−0.11	1.7	0.95
20-1	20	1.4	2.1	0.61
20-2	20	0.23	0.47	0.65

[a] k_G was calculated by plotting $\ln(N_{G,t}/N_{G,0})$ as a function of time for each experiment and calculating the slope, its standard error, and its p value (eq 5), and units for k_G are day^{-1}.

Persistence of Intact HuNoV. For a subset of experiments (experiments 15-2 and 20-2), HuNoV capsid cleavage was assessed by treating samples with RNase prior to RNA extraction to digest gRNA not protected by an intact HuNoV capsid. No significant decay was observed for all genome segments after RNase pretreatment (k values were not significantly different from 0; Figure 1 and Table S11).

DISCUSSION

This study fills an important knowledge gap on the persistence of human norovirus in the environment by presenting new first-order decay rate constants (hereafter, "k values"). We found that the k values varied not significantly different from 0 to 2.2 day^{-1} for infectious HuNoV incubated in filter-sterilized creek water. These k values correspond to a time for 90% (T_{90}) inactivation as fast as 1.1 days; the upper limit for T_{90} could not be determined since k was not significantly different from 0 for one experiment. The range of k values compares well to those of other viruses measured using culture-based methods under dark conditions in environmental water, including nonenveloped viruses, such as other caliciviruses, and bacteriophage, such as MS2. For example, a recent review and meta-analysis of mammalian viruses in environmental water under dark conditions identified a range from 0.00085 day^{-1} (Coxsackievirus A9 in estuarine water incubated at 15 °C[51]) to 7.89 day^{-1} (Coxsackievirus A13 in freshwater incubated at 25 °C[52]), which corresponds to a wide range in T_{90} (from over 7 years to <1 day).[17] A recent study conducted experiments similar to those described herein and found that HuNoV suspended in lake water, drinking water, and ultrapure water incubated at room temperature in the dark had k values within the range we observed from 0.08 to 0.11 day^{-1} or a T_{90} from 21 to 29 days.[25] A human ingestion study found that infectious HuNoV (GI) incubated in groundwater for 61 days at room temperature still caused illness.[53]

We found that incubation temperature (i.e., 20 °C compared to 15 °C) did not explain variation in persistence of infectious HuNoV, but HuNoV genome segments persisted longer at a higher temperature tested in this study. Temperature has been identified to have a significant positive effect on k values for a variety of mammalian viruses in environmental waters: viruses persist longer at lower temperatures.[17] In contrast, in this study, HuNoV genome segments persisted longer at 20 °C compared to 15 °C. It should be noted that the experiments at different temperatures were completed using different strains of HuNoV and creek water collected on different dates. We do not expect that strain-level differences affected the outcome of these experiments but cannot rule out that possibility. Variable constituents in the creek water could have affected these findings.

We observed a large difference between HuNoV k values when the virus was incubated in water collected from the same location on different dates and stored at the same incubation temperature (for example, 2.2 compared to 0.36 ± 0.083 day^{-1} for water stored at 15 °C). This variability has also been demonstrated for infectious HuNoV (GII.4) persistence in seawater, where HuNoV seeded into filter-sterilized seawater and was detectable via the HIE assay for between 7 and 14 days in one sample and for at least 35 days in another from the same location (no k values were reported).[24] These findings suggest that k values may vary greatly within environmental sample matrices; the cause is not clear but could be due to the transient presence of variable constituents in the environmental matrix, which could be biotic (e.g., enzymatic) or abiotic.

For HuNoV genome segments, regardless of length, results ranged from no significant decay observed to a k value of 0.12 ± 0.016 day^{-1}. The k values observed are similar in magnitude to what has been previously reported for HuNoV (GII) seeded into river water and incubated at 25 °C (0.037 day^{-1}) and HuNoV (GI) seeded into surface water and incubated at 25 °C (0.18 day^{-1}), both under dark conditions.[17,19,20] HuNoV infectivity is difficult and costly to assess,[30] and PCR-based methods are commonly applied to infer the occurrence of HuNoV in environmental waters.[14] Generally, RT-qPCR is used to amplify a short HuNoV segment (~100 nt) relative to the size of the HuNoV genome (~7600 nt),[29] and both active and inactive viruses are quantified.[54] This study included short (89 nt) and long (~500 nt) HuNoV genome segments, which had similar overall rates of decay. In this study, HuNoV genome segments persisted longer than infectious HuNoV, which has been observed previously for other mammalian viruses,[17] and was noted in a recent study for HuNoV.[25] These findings indicate that k values for genome segments of HuNoV are conservative proxies for infectious virus k values.

By comparing k values obtained using the genome-wide extrapolation approach, the RNase pretreatment (which measures gRNA inside intact viral capsids), and the HIE assay, it is possible to infer information about mechanisms of inactivation of HuNoV. For experiments 15-2 and 20-2, both the genome-wide k value and k values obtained by measuring intact HuNoV capsids were not significantly different from 0. At the same time, these experiments had k values of 0.21 ± 0.056 and 0.36 ± 0.083 day^{-1} for infectious HuNoV. This finding suggests that, in those experiments, genome damage and capsid cleavage cannot explain the loss of viral infectivity.

https://doi.org/10.1021/acs.est.2c09637
Environ. Sci. Technol. 2023, 57, 3671−3679

It is possible that the loss of viral infectivity in those cases can be explained by damage to the capsid that interfered with virus adhesion to host cells (but not severe enough to allow penetration of RNase), damage to other proteins needed for replication, or damage to the HuNoV genome that was not covered by the RT-qPCR targets applied in this study. For experiment 15-1, the experiment for which we observed the largest k value for infectious HuNoV (2.2 day^{-1}), the genome-wide k value was the same order of magnitude as that derived using the infectivity assay. In this experiment (15-1), we did not measure capsid damage, and only two time points were used to estimate the k value for the HIE experiment, which resulted in uncertainty in that k value of virus inactivation. Despite these limitations, the similarities between the magnitudes of the genome-wide k value and the k value for infectious HuNoV suggest that genome damage was likely a dominant mechanism of inactivation of HuNoV in experiment 15-1. San Pedro Creek drains a highly urbanized catchment and could contain any number of contaminants from automobiles or business and residential units that might cause genome damage.

The experiments conducted herein were carried out using filter-sterilized water and thus do not include the effect of particle-mediated or microbial-mediated decay of HuNoV in surface waters. Filter sterilization was necessary because the HIE cell line demonstrated cytopathic effects when exposed to raw creek water during initial pilot experiments. Particle−virus interactions have been observed in a waste-stabilization pond, where the highest fraction of HuNoV (GII) was associated with particles that were between 0.45 and 180 μm,[55] and similar particle−virus interactions could be important in surface water. The effect of indigenous bacteria or protists on the decay of HuNoV in surface water could also be significant. For example, Olive et al.[56] identified a temperature- and virus-dependent interaction between microorganisms and the decay of echovirus 11, adenovirus type 2, and bacteriophage H6 in surface water. It is important to note that the relationship between HuNoV measured via the HIE infectivity assay and HuNoV infectious to susceptible humans has yet to be quantified.[25] Recent work indicates that HuNoV can replicate in salivary glands,[57] and human salivary gland cell lines may serve in future studies to assess the loss of infectious HuNoV in more complex environmental matrices.

Environmental Implications. There is a striking lack of knowledge on the fate and transport of viruses in the environment that limits our ability to create effective policies to protect human health. HuNoV, in particular, is a leading cause of gastrointestinal illness globally, can be transmitted via the fecal−oral route, and causes waterborne illness, yet there is little information on its persistence and inactivation in environmental water. This study begins to fill that knowledge gap by providing first-order decay rate constants for infectious norovirus as measured by the HIE assay. Inherent in this work is that the HIE assay measures HuNoV with the ability to infect humans and that the measurements (RT-qPCR quantification of viral genomes pre- and postinfection) can be used to deduce first-order decay rate constants, as has been done previously.[25] The wide range in k values of infectious HuNoV observed in the surface water samples collected at the same site highlights variability in HuNoV persistence that is inherent in a complex environment and for which fate and transport models will need to account: a single k value may be insufficient for modeling virus inactivation in surface waters. This variability can be explained, in part, by different inactivation mechanisms at work in different samples with the same bulk water quality characteristics. In one creek water sample from this study, genome damage was likely a dominant inactivation mechanism, but in other samples from the same creek, loss of HuNoV infectivity could not be attributed to genome damage or capsid cleavage. Inactivation mechanisms of viruses in environmental waters are understudied, and continued work identifying inactivation mechanisms and refining methods to assess inactivation mechanisms in complex environmental systems will inform decay and transport model development.

■ ASSOCIATED CONTENT

Data Availability Statement

Data analysis code and dataset are available through the Stanford Digital Repository (https://doi.org/10.25740/tr061rz9792).

Supporting Information

The Supporting Information is available free of charge at https://pubs.acs.org/doi/10.1021/acs.est.2c09637.

Experimental overview (Figure S1); absorbance of filter-sterilized creek water (Figure S2); gel electrophoresis screening for HuNoV (MK764019) (Figure S3); RT-qPCR screening for HuNoV (MK764019) (Figure S4); gel electrophoresis screening for HuNoV (OL913976) (Figure S5); RT-qPCR screening for HuNoV (OL913976) (Figure S6); compiled individual RT-qPCR standard curves (Figure S7); water quality data (Table S1); summary of RT-qPCR assays (Table S2); master-mix recipes (Table S3); thermal cycling conditions (Table S4); candidate assay standard curve information (Table S5); ORF standard curve information (Table S6); master standard curves (Table S7); multiple linear regression: effect of incubation temperature (i.e., 20 °C compared to 15 °C) on infectious HuNoV (Table S8); multiple linear regression: effect of incubation temperature (i.e., 20 °C compared to 15 °C) on decay of HuNoV genome segments (Table S9); multiple linear regression: effect of amplicon length on decay of HuNoV genome segments (Table S10); compiled k values by experiment (Table S11) (PDF)

■ AUTHOR INFORMATION

Corresponding Author

Alexandria B. Boehm − *Department of Civil and Environmental Engineering, Stanford University, Stanford, California 94305, United States;* orcid.org/0000-0002-8162-5090; Email: aboehm@stanford.edu

Authors

Lauren C. Kennedy − *Department of Civil and Environmental Engineering, Stanford University, Stanford, California 94305, United States;* orcid.org/0000-0002-4451-2361

Veronica P. Costantini − *Division of Viral Diseases, Centers for Disease Control and Prevention, Atlanta, Georgia 30329, United States*

Kimberly A. Huynh − *Division of Viral Diseases, Centers for Disease Control and Prevention, Atlanta, Georgia 30329, United States*

Stephanie K. Loeb − *Department of Civil and Environmental Engineering, Stanford University, Stanford, California 94305, United States; Department of Civil Engineering, McGill University, Montreal, QB H3A 0C3, Canada;* orcid.org/0000-0002-8666-518X

Wiley C. Jennings − *Department of Civil and Environmental Engineering, Stanford University, Stanford, California 94305, United States*

Sarah Lowry − *Department of Civil and Environmental Engineering, Stanford University, Stanford, California 94305, United States*

Mia C. Mattioli − *Division of Foodborne, Waterborne, and Environmental Diseases, Centers for Disease Control and Prevention, Atlanta, Georgia 30329, United States*

Jan Vinjé − *Division of Viral Diseases, Centers for Disease Control and Prevention, Atlanta, Georgia 30329, United States*

Complete contact information is available at: https://pubs.acs.org/10.1021/acs.est.2c09637

Notes

The authors declare no competing financial interest.

■ ACKNOWLEDGMENTS

This work was supported by the NSF CBET-1804169 and a grant from the Woods Institute for the Environment at Stanford University.

■ REFERENCES

(1) Hall, A. J.; Lopman, B. A.; Payne, D. C.; Patel, M. M.; Gastañaduy, P. A.; Vinjé, J.; Parashar, U. D. Norovirus Disease in the United States. *Emerging Infect. Dis.* **2013**, *19*, 1198−1205.

(2) Glass, R. I.; Parashar, U. D.; Estes, M. K. Norovirus Gastroenteritis. *N. Engl. J. Med.* **2009**, *361*, 1776−1785.

(3) Patel, M. M.; Widdowson, M.-A.; Glass, R. I.; Akazawa, K.; Vinjé, J.; Parashar, U. D. Systematic Literature Review of Role of Noroviruses in Sporadic Gastroenteritis. *Emerging Infect. Dis.* **2008**, *14*, 1224−1231.

(4) Ahmed, S. M.; Hall, A. J.; Robinson, A. E.; Verhoef, L.; Premkumar, P.; Parashar, U. D.; Koopmans, M.; Lopman, B. A. Global prevalence of norovirus in cases of gastroenteritis: a systematic review and meta-analysis. *Lancet Infect. Dis.* **2014**, *14*, 725−730.

(5) Boehm, A. B.; Soller, J. A.; Shanks, O. C. Human-Associated Fecal Quantitative Polymerase Chain Reaction Measurements and Simulated Risk of Gastrointestinal Illness in Recreational Waters Contaminated with Raw Sewage. *Environ. Sci. Technol. Lett.* **2015**, *2*, 270−275.

(6) Viau, E. J.; Lee, D.; Boehm, A. B. Swimmer Risk of Gastrointestinal Illness from Exposure to Tropical Coastal Waters Impacted by Terrestrial Dry-Weather Runoff. *Environ. Sci. Technol.* **2011**, *45*, 7158−7165.

(7) Wade, T. J.; Augustine, S. A. J.; Griffin, S. M.; Sams, E. A.; Oshima, K. H.; Egorov, A. I.; Simmons, K. J.; Eason, T. N.; Dufour, A. P. Asymptomatic norovirus infection associated with swimming at a tropical beach: A prospective cohort study. *PLoS One* **2018**, *13*, No. e0195056.

(8) Vanden Esschert, K. L.; Mattioli, M. C.; Hilborn, E. D.; Roberts, V. A.; Yu, A. T.; Lamba, K.; Arzaga, G.; Zahn, M.; Marsh, Z.; Combes, S. M.; Smith, E. S.; Robinson, T. J.; Gretsch, S. R.; Laco, J. P.; Wikswo, M. E.; Miller, A. D.; Tack, D. M.; Wade, T. J.; Hlavsa, M. C. Outbreaks Associated with Untreated Recreational Water — California, Maine, and Minnesota, 2018−2019. *Morb. Mortal. Wkly. Rep.* **2020**, *69*, 781−783.

(9) Soller, J. A.; Bartrand, T.; Ashbolt, N. J.; Ravenscroft, J.; Wade, T. J. Estimating the primary etiologic agents in recreational freshwaters impacted by human sources of faecal contamination. *Water Res.* **2010**, *44*, 4736−4747.

(10) Egorov, A. I.; Converse, R.; Griffin, S. M.; Bonasso, R.; Wickersham, L.; Klein, E.; Kobylanski, J.; Ritter, R.; Styles, J. N.; Ward, H.; Sams, E.; Hudgens, E.; Dufour, A.; Wade, T. J. Recreational water exposure and waterborne infections in a prospective salivary antibody study at a Lake Michigan beach. *Sci. Rep.* **2021**, *11*, No. 20540.

(11) Graciaa, D. S.; Cope, J. R.; Roberts, V. A.; Cikesh, B. L.; Kahler, A. M.; Vigar, M.; Hilborn, E. D.; Wade, T. J.; Backer, L. C.; Montgomery, S. P.; Evan Secor, W.; Hill, V. R.; Beach, M. J.; Fullerton, K. E.; Yoder, J. S.; Hlavsa, M. C. Outbreaks Associated with Untreated Recreational Water — United States, 2000−2014. *Am. J. Transplant.* **2018**, *18*, 2083−2087.

(12) Boehm, A. B.; Graham, K. E.; Jennings, W. C. Can We Swim Yet? Systematic Review, Meta-Analysis, and Risk Assessment of Aging Sewage in Surface Waters. *Environ. Sci. Technol.* **2018**, *52*, 9634−9645.

(13) Van Abel, N.; Mans, J.; Taylor, M. B. Quantitative microbial risk assessment to estimate the health risk from exposure to noroviruses in polluted surface water in South Africa. *J. Water Health* **2017**, *15*, 908−922.

(14) Ekundayo, T. C.; Igere, B. E.; Oluwafemi, Y. D.; Iwu, C. D.; Olaniyi, O. O. Human norovirus contamination in water sources: A systematic review and meta-analysis. *Environ. Pollut.* **2021**, *291*, No. 118164.

(15) Tsai, Y. L.; Tran, B.; Palmer, C. J. Analysis of viral RNA persistence in seawater by reverse transcriptase-PCR. *Appl. Environ. Microbiol.* **1995**, *61*, 363−366.

(16) Dancer, D.; Rangdale, R. E.; Lowther, J. A.; Lees, D. N. Human Norovirus RNA Persists in Seawater under Simulated Winter Conditions but Does Not Bioaccumulate Efficiently in Pacific Oysters (Crassostrea gigas). *J. Food Prot.* **2010**, *73*, 2123−2127.

(17) Boehm, A. B.; Silverman, A. I.; Schriewer, A.; Goodwin, K. Systematic review and meta-analysis of decay rates of waterborne mammalian viruses and coliphages in surface waters. *Water Res.* **2019**, *164*, No. 114898.

(18) Silverman, A. I.; Boehm, A. B. Systematic Review and Meta-Analysis of the Persistence of Enveloped Viruses in Environmental Waters and Wastewater in the Absence of Disinfectants. *Environ. Sci. Technol.* **2021**, *55*, 14480−14493.

(19) Ngazoa, Es.; Fliss, I.; Jean, J. Quantitative study of persistence of human norovirus genome in water using TaqMan real-time RT-PCR. *J. Appl. Microbiol.* **2008**, *104*, 707−715.

(20) Bae, J.; Schwab, K. J. Evaluation of Murine Norovirus, Feline Calicivirus, Poliovirus, and MS2 as Surrogates for Human Norovirus in a Model of Viral Persistence in Surface Water and Groundwater. *Appl. Environ. Microbiol.* **2008**, *74*, 477−484.

(21) Elmahdy, M. E. I.; Magri, M. E.; Garcia, L. A.; Fongaro, G.; Barardi, C. R. M. Microcosm environment models for studying the stability of adenovirus and murine norovirus in water and sediment. *Int. J. Hyg. Environ. Health* **2018**, *221*, 734−741.

(22) Moresco, V.; Damazo, N. A.; Barardi, C. R. M. Thermal and temporal stability on the enteric viruses infectivity in surface freshwater. *Water Supply* **2016**, *16*, 620−627.

(23) Ibrahim, E. M. E.; El-Liethy, M. A.; Abia, A. L. K.; Hemdan, B. A.; Shaheen, M. N. Survival of E. coli O157:H7, Salmonella Typhimurium, HAdV2 and MNV-1 in river water under dark conditions and varying storage temperatures. *Sci. Total Environ.* **2019**, *648*, 1297−1304.

(24) Desdouits, M.; Polo, D.; Le Mennec, C.; Strubbia, S.; Zeng, X.-L.; Ettayebi, K.; Atmar, R. L.; Estes, M. K.; Le Guyader, F. S. Use of Human Intestinal Enteroids to Evaluate Persistence of Infectious Human Norovirus in Seawater. *Emerging Infect. Dis.* **2022**, *28*, 1475−1479.

(25) Shaffer, M.; Huynh, K.; Costantini, V.; Bibby, K.; Vinjé, J. Viable Norovirus Persistence in Water Microcosms. *Environ. Sci. Technol. Lett.* **2022**, *9*, 851−855.

(26) Block, J.-C. *Viral Pollution of the Environment*; CRC Press, 1983.

(27) Gerba, C. P. *Perspectives in Medical Virology*; Bosch, A., Ed.; Elsevier, 2007; Vol. *17*, pp 91−108.
(28) Nelson, K. L.; Boehm, A. B.; Davies-Colley, R. J.; Dodd, M. C.; Kohn, T.; Linden, K. G.; Liu, Y.; Maraccini, P. A.; McNeill, K.; Mitch, W. A.; Nguyen, T. H.; Parker, K. M.; Rodriguez, R. A.; Sassoubre, L. M.; Silverman, A. I.; Wigginton, K. R.; Zepp, R. G. Sunlight-mediated inactivation of health-relevant microorganisms in water: a review of mechanisms and modeling approaches. *Environ. Sci.: Processes Impacts* **2018**, *20*, 1089−1122.
(29) Knight, A.; Li, D.; Uyttendaele, M.; Jaykus, L.-A. A critical review of methods for detecting human noroviruses and predicting their infectivity. *Crit. Rev. Microbiol.* **2013**, *39*, 295−309.
(30) Ettayebi, K.; Tenge, V. R.; Cortes-Penfield, N. W.; Crawford, S. E.; Neill, F. H.; Zeng, X.-L.; Yu, X.; Ayyar, B. V.; Burrin, D.; Ramani, S.; Atmar, R. L.; Estes, M. K. New Insights and Enhanced Human Norovirus Cultivation in Human Intestinal Enteroids. *mSphere* **2021**, *6*, No. e01136-20.
(31) Pecson, B. M.; Ackermann, M.; Kohn, T. Framework for Using Quantitative PCR as a Nonculture Based Method To Estimate Virus Infectivity. *Environ. Sci. Technol.* **2011**, *45*, 2257−2263.
(32) Manuel, C. S.; Moore, M. D.; Jaykus, L.-A. Predicting human norovirus infectivity - Recent advances and continued challenges. *Food Microbiol.* **2018**, *76*, 337−345.
(33) Rodríguez, R. A.; Pepper, I. L.; Gerba, C. P. Application of PCR-Based Methods To Assess the Infectivity of Enteric Viruses in Environmental Samples. *Appl. Environ. Microbiol.* **2009**, *75*, 297−307.
(34) Tian, P.; Yang, D.; Shan, L.; Li, Q.; Liu, D.; Wang, D. Estimation of Human Norovirus Infectivity from Environmental Water Samples by In Situ Capture RT-qPCR Method. *Food Environ. Virol.* **2018**, *10*, 29−38.
(35) Loeb, S. K.; Jennings, W. C.; Wigginton, K. R.; Boehm, A. B. Sunlight Inactivation of Human Norovirus and Bacteriophage MS2 Using a Genome-Wide PCR-Based Approach and Enzyme Pretreatment. *Environ. Sci. Technol.* **2021**, *55*, 8783−8792.
(36) Lee, H.-W.; Lee, H.-M.; Yoon, S.-R.; Kim, S. H.; Ha, J.-H. Pretreatment with propidium monoazide/sodium lauroyl sarcosinate improves discrimination of infectious waterborne virus by RT-qPCR combined with magnetic separation. *Environ. Pollut.* **2018**, *233*, 306−314.
(37) Gyawali, P.; Hewitt, J. Detection of Infectious Noroviruses from Wastewater and Seawater Using PEMAXTM Treatment Combined with RT-qPCR. *Water* **2018**, *10*, 841.
(38) Oristo, S.; Lee, H. J.; Manula, L. Performance of pre-RT-qPCR treatments to discriminate infectious human rotaviruses and noroviruses from heat-inactivated viruses: applications of PMA/PMAxx, benzonase and RNase. *J. Appl. Microbiol.* **2018**, *124*, 1008−1016.
(39) Wanders, N.; van Vliet, M. T. H.; Wada, Y.; Bierkens, M. F. P.; Rens van Beek, L. P. H. High-Resolution Global Water Temperature Modeling. *Water Resour. Res.* **2019**, *55*, 2760−2778.
(40) Gerba, C. P.; Betancourt, W. Q. Viral Aggregation: Impact on Virus Behavior in the Environment. *Environ. Sci. Technol.* **2017**, *51*, 7318−7325.
(41) Walters, S. P.; Gonzalez-Escalona, N.; Son, I.; Melka, D. C.; Sassoubre, L. M.; Boehm, A. B. Salmonella enterica Diversity in Central Californian Coastal Waterways. *Appl. Environ. Microbiol.* **2013**, *79*, 4199−4209.
(42) Li, D.; Baert, L.; Xia, M.; Zhong, W.; Van Coillie, E.; Jiang, X.; Uyttendaele, M. Evaluation of methods measuring the capsid integrity and/or functions of noroviruses by heat inactivation. *J. Virol. Methods* **2012**, *181*, 1−5.
(43) Topping, J. R.; Schnerr, H.; Haines, J.; Scott, M.; Carter, M. J.; Willcocks, M. M.; Bellamy, K.; Brown, D. W.; Gray, J. J.; Gallimore, C. I.; Knight, A. I. Temperature inactivation of Feline calicivirus vaccine strain FCV F-9 in comparison with human noroviruses using an RNA exposure assay and reverse transcribed quantitative real-time polymerase chain reaction-A novel method for predicting virus infectivity. *J. Virol. Methods* **2009**, *156*, 89−95.
(44) Dunkin, N.; Weng, S.; Coulter, C. G.; Jacangelo, J. G.; Schwab, K. J. Reduction of Human Norovirus GI, GII, and Surrogates by Peracetic Acid and Monochloramine in Municipal Secondary Wastewater Effluent. *Environ. Sci. Technol.* **2017**, *51*, 11918−11927.
(45) Costantini, V.; Morantz, E. K.; Browne, H.; Ettayebi, K.; Zeng, X.-L.; Atmar, R. L.; Estes, M. K.; Vinjé, J. Human Norovirus Replication in Human Intestinal Enteroids as Model to Evaluate Virus Inactivation. *Emerging Infect. Dis.* **2018**, *24*, 1453−1464.
(46) Borchardt, M. A.; Boehm, A. B.; Salit, M.; Spencer, S. K.; Wigginton, K. R.; Noble, R. T. The Environmental Microbiology Minimum Information (EMMI) Guidelines: qPCR and dPCR Quality and Reporting for Environmental Microbiology. *Environ. Sci. Technol.* **2021**, *55*, 10210−10223.
(47) Loisy, F.; Atmar, R. L.; Guillon, P.; Le Cann, P.; Pommepuy, M.; Le Guyader, F. S. Real-time RT-PCR for norovirus screening in shellfish. *J. Virol. Methods* **2005**, *123*, 1−7.
(48) Chick, H. An Investigation of the Laws of Disinfection. *J. Hyg.* **1908**, *8*, 92−158.
(49) *Interaction Effects in Multiple Regression*; SAGE Publications, Inc., Thousand Oaks, 2022.
(50) Yang, H.; Min, X.; Wu, J.; Lin, X.; Gao, F.-Z.; Hu, L.-X.; Zhang, L.; Wang, Y.; Xu, S.; Ying, G.-G. Removal and Inactivation of Virus by Ceramic Water Filters Coated with Lanthanum (III). *ACS EST Water* **2022**, *2*, 1811−1821.
(51) Nasser, A. M.; Zaruk, N.; Tenenbaum, L.; Netzan, Y. Comparative survival of Cryptosporidium, coxsackievirus A9 and Escherichia coli in stream, brackish and sea waters. *Water Sci. Technol.* **2003**, *47*, 91−96.
(52) O'Brien, R. T.; Newman, J. S. Inactivation of polioviruses and coxsackieviruses in surface water. *Appl. Environ. Microbiol.* **1977**, *33*, 334−340.
(53) Seitz, S. R.; Leon, J. S.; Schwab, K. J.; Lyon, G. M.; Dowd, M.; McDaniels, M.; Abdulhafid, G.; Fernandez, M. L.; Lindesmith, L. C.; Baric, R. S.; Moe, C. L. Norovirus Infectivity in Humans and Persistence in Water ∇. *Appl. Environ. Microbiol.* **2011**, *77*, 6884−6888.
(54) Richards, G. P. Limitations of Molecular Biological Techniques for Assessing the Virological Safety of Foods. *J. Food Prot.* **1999**, *62*, 691−697.
(55) Silva, A. K. d.; Guyader, F. S. L.; Saux, J.-C. L.; Pommepuy, M.; Montgomery, M. A.; Elimelech, M. Norovirus Removal and Particle Association in a Waste Stabilization Pond. *Environ. Sci. Technol.* **2008**, *42*, 9151−9157.
(56) Olive, M.; Gan, C.; Carratalà, A.; Kohn, T. Control of Waterborne Human Viruses by Indigenous Bacteria and Protists Is Influenced by Temperature, Virus Type, and Microbial Species. *Appl. Environ. Microbiol.* **2020**, *86*, No. e01992-19.
(57) Ghosh, S.; Kumar, M.; Santiana, M.; Mishra, A.; Zhang, M.; Labayo, H.; Chibly, A. M.; Nakamura, H.; Tanaka, T.; Henderson, W.; Lewis, E.; Voss, O.; Su, Y.; Belkaid, Y.; Chiorini, J. A.; Hoffman, M. P.; Altan-Bonnet, N. Enteric viruses replicate in salivary glands and infect through saliva. *Nature* **2022**, *607*, 345−350.

https://doi.org/10.1021/acs.est.2c09637
Environ. Sci. Technol. 2023, 57, 3671−3679